IDLE SPEED CONTROL OF PORT-INJECTION ENGINES VIA THE POLYNOMIAL EQUATION APPROACH

Leonardo Albertoni [*] **Andrea Balluchi** [**]
Alessandro Casavola [***] **Claudio Gambelli** [*]
Edoardo Mosca [*]
Alberto L. Sangiovanni–Vincentelli [**,****]

[*] *Dip. di Sistemi ed Informatica, Università di Firenze*
Via S.Marta, 3 - 50139 Firenze, Italy.
Email: {albertoni,gambelli,mosca}@dsi.unifi.it
[**] *PARADES, Via San Pantaleo, 66 - 00186 Roma, Italy.*
Email: {balluchi,alberto}@parades.rm.cnr.it
[***] *Dip. di Elettronica, Informatica e Sistemistica,*
Università della Calabria, Arcavacata di Rende - (CS),
87037 Italy. Email: casavola@si.deis.unical.it
[****] *EECS Dept., University of California at Berkeley*
CA 94720, USA. Email: alberto@eecs.berkeley.edu

Abstract: The design of an idle speed controller for automotive engines is considered. A hybrid nonlinear model of the engine is presented. Based on suitable (nonlinear) change of variables, the idle speed control design problem can satisfactorily be addressed via LTI techniques. Specifically, the design problem has been formalized as a finite dimensional discrete-time ℓ_∞ optimal control problem, whereby the fuel consumption has to be minimized. Polynomial techniques have been used to convert the control design formulation to a linear "least absolute data fitting" problem, for which solution very efficient and stable numerical methods exist. Experimental results on a commercial car have been finally reported.

Keywords: Automotive idle-speed control, engine control, polynomial methods, ℓ_∞ control, dead-beat control.

1. INTRODUCTION

The main targets of the design of gasoline engines for passenger cars are: improvement of safety and driveability, minimization of fuel consumption and compliance with the emission standards. The difficulty of controlling the engine at idle is due to the variation of the torque absorbed by the devices powered by the engine, such as the air conditioning system and the steering wheel servo-mechanism, which may cause engine stall. Interesting results on idle speed control have been presented in (Balluchi *et al.*, 2000; Hrovat and Sun, 1997; Butts *et al.*, 1999; Shim *et al.*, 1996; Yurkovich and M.Simpson, 1997; Carnevale and Moschetti, 1993). A hybrid formalism is adopted here to describe the cyclic behavior of the engine. Such formalism is particularly useful for validation purposes. In fact, since at idle speed the frequency of the engine cycles is very low, then an improper control action – even for a single engine cycle – may cause the engine to stall. Nevertheless, LTI techniques can be used for control design

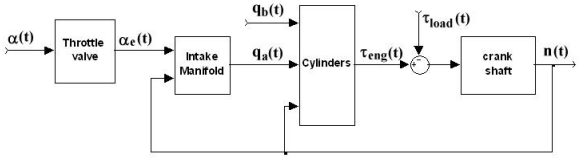

Fig. 1. Hybrid engine model.

purposes because, at idle, the dynamic ranges of all system variables of interest are small and linearization techniques are effective. Moreover, we have adopted a suitable (nonlinear) change of variables and an ad-hoc control structure (patent pending), which have contributed to make the problem affordable by standard LTI control techniques. Certainly, fuel consumption minimization is paramount at idle. However, also fast rejection of load step disturbances is important and should be guaranteed to a certain extent. To this end, the idle speed control problem is formalized as a finite dimensional ℓ_∞ optimal control problem, which is solved via polynomial techniques. Specifically, the parameterization of all closed-loop ripple-free dead-beat responses to step disturbances is used to characterize the corresponding class of stabilizing controllers over which the fuel consumption is minimized in a ℓ_∞ sense. The performance of the proposed controller has been tested in extensive simulations of the hybrid closed-loop model. Experimental results on a commercial car are reported and testify the effectiveness of the design approach. Significant improvements in terms of disturbance rejection, idle speed fluctuation and fuel consumption have been achieved with respect to the standard PID/LQ controllers, traditionally adopted in the automotive industry.

2. HYBRID ENGINE MODEL

In this section, a nonlinear hybrid model of a 4–stroke 4–cylinder spark ignition engine for idle speed control is briefly presented (see (Albertoni *et al.*, 2003; Balluchi *et al.*, 2000) for more details). Engine control inputs are:

- The throttle valve command α, used to control the engine air charge q_a;
- The spark advance angle β, which defines the ignition timing.

Fuel injection is set according to the evolution of the air charge q_a so as to ensure a stoichiometric ratio to the mixture, as requested for tailpipe emission control.

As depicted in Fig. 1, the engine hybrid model is composed of: the *throttle valve*, the *intake manifold*, the *cylinders* and the *crankshaft*. The *throttle valve* model is

$$\dot{\alpha_e}(t) = \frac{1}{\tau_\alpha}\alpha_e(t) + \frac{1}{\tau_\alpha}\alpha(t - d_\alpha) \qquad (1)$$

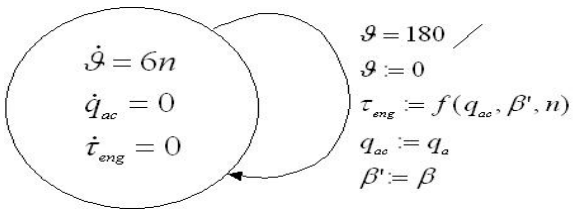

Fig. 2. Hybrid model of the cylinders.

where: α and α_e denote, respectively, the throttle valve command and the throttle valve angle; d_α models the actuator delay. The *intake manifold* dynamics is described in terms of the intake manifold pressure p as follows:

$$\dot{p}(t) = K_g[F_{th}(p(t), \alpha_e(t)) - F_{cyl}(p(t), n(t))] \quad (2)$$

$$q_a(t) = \frac{k_1}{n} F_{cyl}(p(t), n(t)) \qquad (3)$$

where F_{th} denotes the air–flow rate through the throttle valve and F_{cyl} denotes the cylinder air–flow rate (the latter depending on the crankshaft speed n). Let t_k^{dc} denote the sequence of time instants at which the pistons reach a dead center, i.e. either the lower most (bottom dead center) or the upper most (top dead center) positions. The output equation (3), evaluated at time $t = t_k^{dc}$, gives the amount of air mass $q_a(k) = q_a(t_k^{dc})$ loaded by the cylinder that concluded the intake stroke at time t_k^{dc}. Fig. 2 reports the hybrid model of the *cylinders*, which describes the torque generation mechanism for 4–cylinder engines. In this model, the end of a stroke and the beginning of the subsequent one is represented by the dead–center self–loop transition, that is executed when the crankshaft angle θ reaches 180 degrees. This transition defines the dead–center time sequence t_k^{dc}. The crankshaft angle dynamics is

$$\dot{\theta}(t) = k_N\ n(t), \text{with reset } \theta := 0 \text{ when } \theta = 180.$$

The torque generated by the engine during the k–th expansion stroke depends on: the spark advance command $\beta(t_{k-1}^{dc})$ (set at the beginning of the compression stroke), the mass of loaded air $q_a(t_{k-1}^{dc})$, and the engine speed at the beginning of the expansion stroke $n(t_k^{dc})$ (see Fig. 3). The engine torque, $T_{eng}(t)$, is modeled as a piece–wise constant signal, with discontinuity points at times t_k^{dc}, synchronized with the dead center events, i.e.

$$T_{eng}(t) = T_{pot}(q_a(t_{k-1}^{dc}), n(t_k))\, \eta(\beta(t_{k-1}^{dc})) \quad (4)$$

for $t \in [t_k, t_{k+1})$. In (4), $\eta(\cdot) \in [0.6, 1]$ is the *spark ignition efficiency* and T_{pot} is the *potential engine torque*, which is really delivered when $\eta = 1$. Finally, the *crankshaft* model describes the evolution of the crankshaft revolution speed n,

$$\dot{n}(t) = K_J(T_{eng}(t) - T_{load}(t))\ . \qquad (5)$$

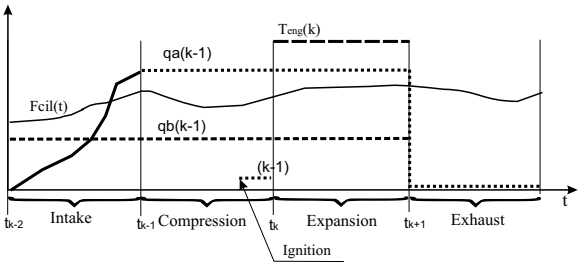

Fig. 3. Delays in engine torque generation.

In (5), T_{load} models the load torque acting on the crankshaft, which is due to pumping and friction losses and auxiliary subsystems powered by the engine (e.g. electric generator and steering pump).

3. MULTIRATE ENGINE MODEL FOR CONTROLLER SYNTHESIS

The engine control unit is equipped with spark ignition and intake throttle valve controllers, each one guaranteeing a good tracking of reference signals T_{ec} and T_{pc}, respectively, for the engine torque T_{eng} and the potential torque T_{pot}. See Fig. 4. Such inner–loop controllers include appropriate compensation of nonlinearities and have been designed and validated on the basis of the hybrid engine model presented in Section 2. In addition, a feedforward filter is used to compute an estimate T_{pe} of the actual potential torque T_{pot}, according to (4). For synthesis purposes, the partially controlled engine can be represented as a multirate system composed of two SISO discrete-time plants (see (Albertoni *et al.*, 2003)). By introducing the unitary delay operator d, defined as $dy(t) := y(t-1)$, the engine model can be rewritten as follows:

$$n(d) = \mathcal{P}_1(d)T_{ec}(d) + \mathcal{P}_{1d}(d)T_{load}(d) \quad (6)$$

$$T_{pe}(d) = \mathcal{P}_2(d)T_{pc}(d) \quad (7)$$

with

$$\mathcal{P}_1(d) = \frac{B_1(d)}{A_1(d)},\ \mathcal{P}_2(d) = \frac{B_2(d)}{A_2(d)},\ \mathcal{P}_{1d}(d) = \frac{C_1(d)}{A_1(d)}$$

and (A_1, B_1), (A_1, C_1) and (A_2, B_2) coprime polynomial pairs. The dynamics (6) models the evolution of the crankshaft speed at the dead-center times, which depends on the reference engine torque T_{ec} and the load torque T_{load}. This model is obtained from (4–5) and it is valid as long as the spark advance command does not saturate, i.e. for $T_{ec} \leq T_{pc}$. The time interval between two subsequent dead–centers is not uniform since it depends on the engine speed n. However, to simplify the synthesis, we assume a constant dead–center period $Tc_1 = 44\ ms$, corresponding to the nominal engine speed $n_0 = 680\ rpm$. Robustness of the controller with respect to dead–center time variations is discussed in (Balluchi *et al.*, 2005). The dynamics (7) is related to the air charge control and has a fixed sampling time $Tc_2 = 12ms$. By controlling the air charge, T_{pc} in (4) is modulated so as to avoid saturation of the spark ignition efficiency η.

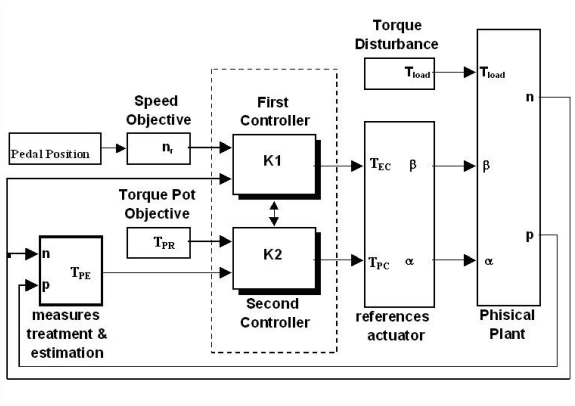

Fig. 4. System Structure.

4. CONTROLLER SYNTHESIS

The proposed controller structure, depicted in Fig. 4, consists of two SISO controllers. The first one is the *Spark-Advance Ignition Reference* controller $\mathcal{K}_1(d)$, used to control the engine speed dynamics (6) to the speed reference signal n_r, obtained from the gas pedal position. Its main goal is a fast rejection of step disturbances T_{load}. To reduce fuel consumption, a low activity of the command T_{ec} is also required. The second controller is the *Air-Mass Reference* controller $\mathcal{K}_2(d)$, in charge of regulating the dynamics (7) to the potential torque reference signal T_{pr}, introduced for feedforward compensation of torque loads. Its main objective is to provide a good tracking of T_{pr} by T_{pe}, with strict requirements on rise-time and overshoot. This controller contributes to avoid saturations on the first command T_{ec}. The controllers $\mathcal{K}_1(d)$ and $\mathcal{K}_2(d)$ are described, respectively, in Section 4.1 and Section 4.2 below.

4.1 Spark-Advance Reference controller $\mathcal{K}_1(d)$

Consider the scalar, sampled-data system of Fig. 5. Assuming for simplicity $r(k) = 0$,

$$Y(d) = \frac{B(d)}{A(d)}U(d) + \frac{C(d)}{A(d)}D(d)\ , \quad (8)$$

where: $U(d)$, $Y(d)$ and $D(d)$ stand for the $\mathcal{D}$-transforms of, respectively, the input, the output and the disturbances sequences $u(t)$, $y(t)$ and d(t); $\frac{B(d)}{A(d)}$ and $\frac{C(d)}{A(d)}$ are, respectively, strictly causal and causal transfer functions given as ratio of

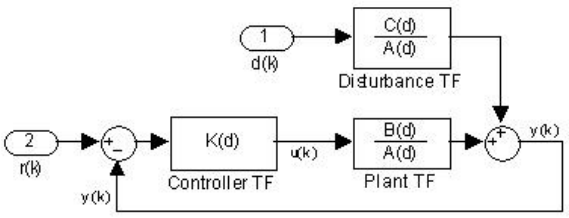

Fig. 5. First Feedback control structure.

polynomials A, B and C. Assume that the disturbance sequence $d(t)$ is a polynomially unbounded sequence with rational $\mathcal{D}$-transform

$$D(d) := \frac{B_d(d)}{A_d(d)} \tag{9}$$

with roots of $A_d(d)$ in $|d| \geq 1$. Notice that (9) includes any non decreasing sequence as step or ramp signals. Assume also:

$$(\mathbf{A.1}) \begin{cases} (A, B) \text{ coprime with } A(0) \neq 0,\ B(0) = 0 \\ (A_d, B_d) \text{ coprime with } A_d(0) \neq 0. \end{cases}$$

Define the feedback action between the output $y(t)$ and $u(t)$ as $U(d) = -\mathcal{K}(d)Y(d)$ with

$$\mathcal{K}(d) = \frac{S(d) + A(d)\mathcal{Q}(d)}{R(d) - B(d)\mathcal{Q}(d)} \ . \tag{10}$$

It is well known (Kučera, 1979) that $\mathcal{K}(d)$ in (10) represents the class of all stabilizing controllers for (8) provided that the polynomial pair (R, S) satisfies the following Bezout equation

$$A(d)R(d) + B(d)S(d) = 1 \ , \tag{11}$$

with the free transfer function $\mathcal{Q}$ causal and asymptotically stable. Because of coprimeness of (A, B), (11) is always solvable with $\deg S < \deg A$ and $\deg R < \deg B$. For the design, we will exploit dead-beat ripple-free output responses, viz $Y(d)$ and $\Delta U(d) := (1 - d)U(d)$ both polynomials (Franklin and Emami-Naemi, 1986). To determine $\mathcal{Q}(d)$, let the polynomials B, A_d, B_d and C be partitioned as the product of stable/antistable terms: $B = B^-B^+$, $A_d = A_d^-A_d^+$, $B_d = B_d^-B_d^+$ and $C = C^-C^+$, where B^+ is a strictly stable polynomial (i.e. free of roots in $|d| \leq 1$) and B^- is a monic unstable polynomial (with all of its roots in $|d| \leq 1$), and so on for the other polynomials. It is further assumed:

$$(\mathbf{A.2}) \begin{cases} (A_d, B) \text{ coprime polynomial pair} \\ A_d \text{ factor of } (1 - d)C^-, \text{ i.e.} \\ (1 - d)C^- = GA_d, \text{ for some polynomial } G. \end{cases}$$

The first assumption is required to ensure both the dead-beat and ripple-free properties, whereas the second is needed only if ripple-free responses are of interest. The following complete parameterization is given in (Casavola *et al.*, 1999).

Proposition 1 - Let (A.1)-(A.2) be fulfilled. Then, Youla parameters $\mathcal{Q}$ in (10), yielding all ripple-free dead–beat controllers, and the corresponding closed-loop responses $Y(d)$ and $\Delta U(d)$ can be parameterized in terms of an arbitrary polynomial $W(d)$ as follows

$$\mathcal{Q} = \frac{Z_o + A_d\,(T_o + B^+W)}{C^+B^+B_d^+} \tag{12}$$

$$Y = Y^o - C^-B^-B_d^-[T_o + B^+W] \tag{13}$$

$$\Delta U = GB_d^-\left(SC^+B_d^+ + A\,[V_o + A_dW]\right) \tag{14}$$

with G as in (A.2)

where: (Y_o, Z_o) is the unique minimal degree solution with respect to Y (i.e. $\deg Y < \deg C^-B^-B_d^-$) of the polynomial Diophantine equation

$$CB_dR - A_dY = ZC^-B^-B_d^-$$

while (V_o, T_o) is the unique minimal degree solution with respect to T (i.e. $\deg T_o < \deg B^+$) of the polynomial Diophantine equation

$$-A_dT + B^+V = Z_o \ .$$

Performance analysis. Since the minimization of the control effort is of primary importance, then the following problems are considered

$$\text{(P.3)} \quad \min_{W \in \Re^w[d]} \|\Delta U\|_{\mathcal{A}_\infty}$$

$$\text{(P.4)} \quad \min_{W \in \Re^w[d]} \|\Delta U\|_{\mathcal{A}_\infty}, \text{ subject to } \|Y\|_{\mathcal{A}_\infty} < \gamma_2$$

where $\mathcal{A}_\infty$ denotes the set of all $\mathcal{D}$-transforms of sequences in ℓ_∞, viz. the set of bounded sequences. Given $H(d) := \sum_{k=0}^{\infty} \hat{h}_k d^k$, it results $\|H(d)\|_{\mathcal{A}_\infty} := \|\hat{h}_k\|_\infty$.

It is worth pointing out that the minimization of ΔU is relevant here because it quantifies displacements with respect to steady-state. In fact, under step disturbances, ΔU is nonzero only during transients. Then, (P.3) and (P.4) express the requirement that, among all responses of length w, the one minimizing the maximum displacement from the constant command corresponding to the steady-state has to be preferred. In (P.4), a constraint on the maximum performance error $\|Y\|_{\mathcal{A}_\infty}$ is also considered.

Finally, it is worth noting that (Casavola, 1996; Casavola *et al.*, 1999) showed that $\mathcal{A}_\infty$-norm minimization problems for FIR systems are equivalent to linear Chebyschev data fitting (LCDF) problems, which can be efficiently solved by standard LP solvers for any chosen horizon $w := \deg W$.

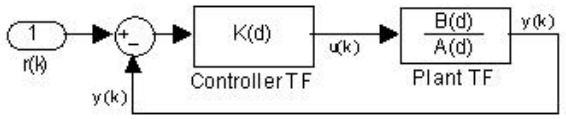

Fig. 6. Second Feedback control structure

4.2 Air-Mass Reference controller $\mathcal{K}_2(d)$

The controller $\mathcal{K}_2(d)$ has been designed via an analytical approach. Consider the scalar, sampled-data system of Fig. 6. Let the desired response from $r(t)$ to $y(t)$ be characterized by the closed-loop transfer fraction

$$\mathcal{W}_0(s) = \frac{\omega_n^2}{s^2 + 2\xi\omega_n s + \omega_n^2}$$

with ω_n and ξ satisfying given rise-time and overshoot specifications. First, $\mathcal{W}_0(s)$ is converted to discrete-time representation, obtaining $\mathcal{W}_0(d) = \frac{N_w(d)}{D_w(d)}$. Then, the identity

$$\mathcal{W}_0(d) = \frac{Y(d)}{U(d)} = \frac{\mathcal{K}(d)\mathcal{P}(d)}{1 + \mathcal{K}(d)\mathcal{P}(d)}$$

is imposed. The controller is obtained as follows

$$\mathcal{K}(d) = \frac{S(d)}{R(d)} = \frac{\mathcal{W}_o(d)}{\mathcal{P}(d) - \mathcal{W}_o(d)} = \frac{N_w A}{(N_w - D_w)B}.$$

If (A, B) are coprime and strictly Hurwitz, then the problem has a unique solution, the closed-loop system is stable and realizes the desired transfer function $\mathcal{W}_0(d)$.

5. EXPERIMENTAL RESULTS

In this section, we report some experimental results obtained in Magneti Marelli Powertrain, Bologna (Italy), by implementing the two SISO control loops illustrated in Section 4 on the ECU of a 1.4L Volkswagen Polo engine. First, the LTI models (6–7) of the partially controlled engine have been identified. The order of the resulting controllers are 5 for $\mathcal{K}_1$ and 3 for $\mathcal{K}_2$. The experimental results show the effectiveness of the proposed controller in terms of both crankshaft speed fluctuation around the nominal set-point and rejection of load step disturbances. Notable improvements on car driveability have been reported by Magneti Marelli Powertrains experts during road tests.

In Fig. 7–10, the following variables are reported for each experiment (from top to down):

- Reference speed engine n_r and measured speed engine n;
- Engine torque command T_{ec};

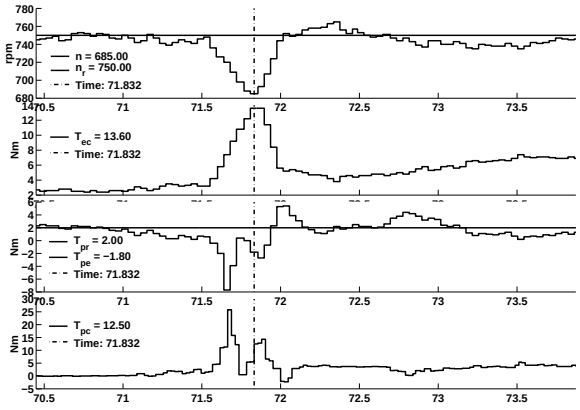

Fig. 7. Response to a step disturbance.

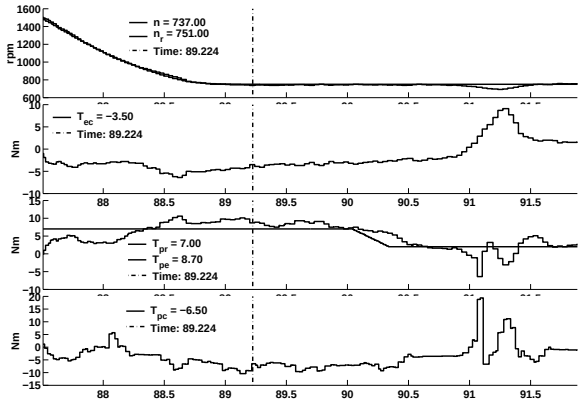

Fig. 8. Transient towards idle.

- Reference potential torque T_{pr} and estimated potential torque T_{pe};
- Potential torque command T_{pc}.

Fig. 7 reports the engine response to a large step load disturbance starting at time $t = 71.5$. The behavior is completely satisfactory: the undershoot has been halved with respect to standard PID/LQ regulators performances; the overshoot is very small and no saturation occurs. In Fig. 8, a transient towards idle is reported. The engine speed n drops from high values to the idle speed value. Also in this case, transients are smooth, fast and well dumped. In fact, only a very low undershoot of 14 rpm can be observed at time $t = 89.2$. In this type of experiments, standard PID/LQ regulators usually exhibit strong undershoots. Fig. 9 reports a very critical test: the system is subject to fast variations of the reference engine speed n_r. Under this type of excitation, standard PID/LQ controllers usually produce large undershoots and oscillations. On the contrary, the behavior of the proposed controller is very good in that neither undershoot nor speed fluctuations are practically observed, while the control effort is small. Finally, Fig. 10 reports the response to a LP–filtered step reference. Even if the synthesis has not been oriented to engine speed tracking performance, the behavior is excellent.

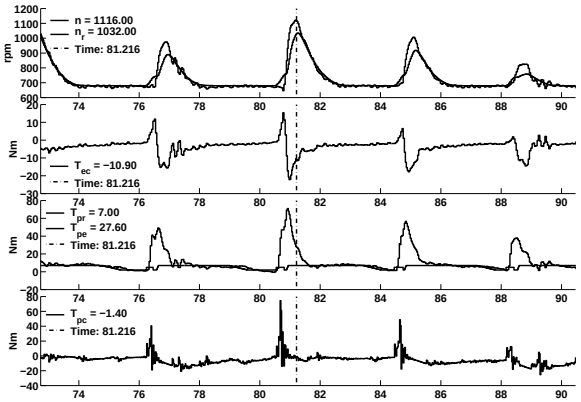

Fig. 9. Rapid variations of the reference speed.

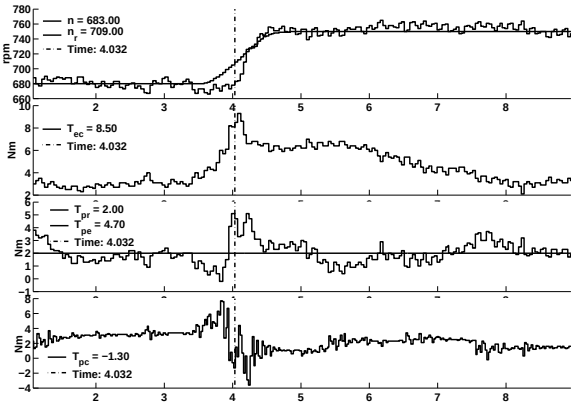

Fig. 10. Tracking of a LP–filtered step reference.

6. CONCLUSION

In this paper, the design of an idle speed controller for an automotive gasoline port-injection engine has been considered. The problem has been formalized as a finite dimensional ℓ_∞ optimization control problem. The polynomial equation approach has been instrumental to the synthesis of the controller. In the proposed solution, implementation constraints related to algorithm complexity are easily handled by choosing the controller order small enough. The proposed controller has been validated by extensive simulations on a hybrid model of the engine. Experimental results show the larger flexibility and effectiveness of the proposed controller with respect to standard PID/LQ controllers in achieving the demanding control objectives. In particular, fast rejection of step load disturbances, low undershoots and limited speed fluctuation have been achieved with relatively low control activity, which in turn implies low fuel consumption.

ACKNOWLEDGMENTS

We thank Magneti Marelli Powertrain, Bologna (Italy) for the support in the development and the experimental work, and in particular Savino Lupo and Giovanni Prodi for the valuable collaboration. This work has been partially supported by the EU Project IST-2001-33520 CC "Control and Computation" and the MIUR Project 2002-04 "Fault Detection and Diagnosis, Control Reconfiguration and Performance Monitoring in Industrial Process".

REFERENCES

Albertoni, L., A. Balluchi, A. Casavola, C. Gambelli, E. Mosca and A. L. Sangiovanni-Vincentelli (2003). Idle speed control for gdi engines using robust multirate hybrid command governors. In: *Proc. CCA2003, 2003 IEEE Conference on Control Applications*. Vol. 1. Istanbul, Turkey. pp. 140–145.

Balluchi, A., L. Benvenuti, M. D. Di Benedetto, C. Pinello and A. L. Sangiovanni-Vincentelli (2000). Automotive engine control and hybrid systems: Challenges and opportunities. *Proceedings of the IEEE* **88**(7), 888–912.

Balluchi, A., P. Murrieri and A. L. Sangiovanni-Vincentelli (2005). Controller synthesis on non–uniform and uncertain discrete–time domains. In: *Hybrid Systems: Computation and Control - HSCC2005*. LNCS. Springer-Verlag.

Butts, K. R., N. Sivashankar and J. Sun (1999). Application of ℓ_1 optimal control to the engine idle speed control problem. *IEEE Trans. on Contr. Syst.s Tech.* **7**(2), 258–270.

Carnevale, C. and A. Moschetti (1993). Idle speed control with H_∞ technique. Technical Report 930770. SAE.

Casavola, A. (1996). A polynomial approach to the l_1 mixed sensitivity optimal control problem. *IEEE Trans.Aut.Contr.* **41**(5), 751–756.

Casavola, A., E. Mosca and P. Zecca (1999). Robust ripple-free deadbeat control design. *International Journal of Control* **72**, 564–573.

Franklin, G.F. and A. Emami-Naemi (1986). Design of ripple-free multivariable robust servomechanisms. *IEEE Trans. Aut. Contr.* **31**, 661–664.

Hrovat, D. and J. Sun (1997). Models and control methodologies for IC engine idle speed control design. *Control Engineering Practice*.

Kučera, V. (1979). *Discrete Linear Control*. Wiley. New York.

Shim, D., J. Park, P. P. Khargonekar and W. B. Ribbens (1996). Reducing automotive engine speed fluctuation at idle. *IEEE Trans. on Contr. Syst.s Tech.* **4**(4), 404–410.

Yurkovich, S. and M.Simpson (1997). Crank-angle domain modeling and control for idle speed. *SAE Journal of Engines* **106**(970027), 34–41.